Speciation analysis and thermodynamic criterion of solvate ionic liquids; whether ionic liquids or super-concentrated solutions?

Nana Arai[a], Hikari Watanabe[a], Erika Nozaki[a], Shiro Seki[b], Seiji Tsuzuki[c], Kazuhide Ueno[d], Kaoru Dokko[d], Masayoshi Watanabe[d], Yasuo Kameda[e] and Yasuhiro Umebayashi[a]*

[a]Graduate School of Science and Technology, Niigata University, 8050 Ikarashi, 2-no-cho, Nishi-ku, Niigata City, 950-2181, Japan,

[b]Department of Environmental Chemistry and Chemical Engineering, School of Advanced Engineering, Kogakuin University, Hachioji City, Tokyo 192-0015, Japan,

[c]Research Center for Computational Design of Advanced Functional Materials (CD-FMat), National Institute of Advanced, Industrial Science and Technology (AIST), Tsukuba Central 2, 1-1-1 Umezono, Tsukuba City, Ibaraki 305-8568, Japan,

[d]Department of Chemistry and Biotechnology, Yokohama National University, 79-5 Tokiwadai, Hodogaya-ku, Yokohama City, Kanagawa 240-8501, Japan,

[e]Department of Material and Biological Chemistry, Faculty of Science, Yamagata University 1-4-12, Kojirakawa-machi, Yamagata City, Yamagata 990-8560, Japan.

- **Detail of compremental linear least squares analysis (CLSA)**

Taking into account the solvation number of solvents n, we obtain following equation,

$$I(\nu) = J_{ub}(\nu)\, c_T \quad + \{J_b(\nu) - \underline{J}_{ub}(\nu)\} \cdot n \cdot c_{Li} \qquad \text{(S1)},$$

where c_{Li} is a lithium salt concentration. In Figure S1, slopes and intercepts correspond to $J_{ub}(\nu)$ and $\{J_b(\nu) - \underline{J}_{ub}(\nu)\} \cdot n \cdot c_{Li}$, respectively. For glyme SILs, $n = 1$, so that the slopes and intercepts directly give $J_{ub}(\nu)$ and $J_b(\nu)$ as a function of ν; the Raman

spectra for *unbound* and *bound* glymes of one moles. Once $J_{ub}(\nu)$ and $J_b(\nu)$ are obtained, then the concentration for the unbound and bound glymes could be parameters in the following equation as variables $J_{ub}(\nu)$ and $J_b(\nu)$:

$$I(\nu) = J_{ub}(\nu) \cdot [\mathrm{ub}] + J_b(\nu) \cdot [\mathrm{b}] \qquad \text{(S2)},$$

First values of $J_{ub}(\nu)$ and $J_b(\nu)$ should contain systematic errors, and thus they should be approximate ones. Therefore, more valid values can be guessed by using adequate peak functions; the *pseudo*-Voigt functions. In this procedure negative values in $J_{ub}(\nu)/J_b(\nu)$ can be avoided. Thus, simple linear regression analysis yields [ub] and [b]; the species distribution functions. Similarly, the species distribution functions can be properly approximate by using polynomials to avoid negative values, then $J_{ub}(\nu)$ and $J_b(\nu)$ can be refined again. These two linear least squares analyses should be complemental, so that they have to be repeated with each other. Hence, these analyses were named as the CLSA.

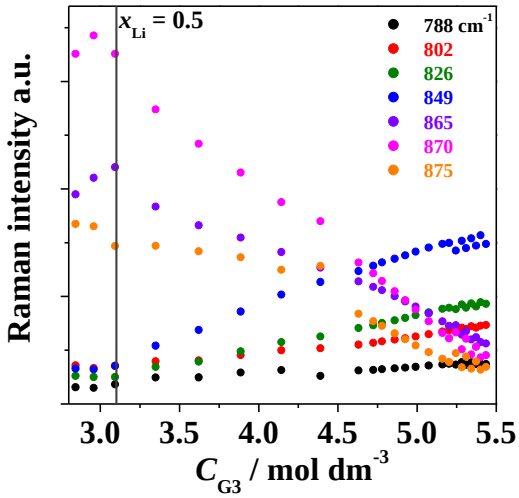

Figure S1. The intensity plots of Raman spectra for G3 in $[\mathrm{LiTFSA}]_x[\mathrm{G3}]_{(1-x)}$ at 298 K at 788 (black), 802 (red), 826 (green), 849 (blue) and 870 (pink) cm^{-1}.

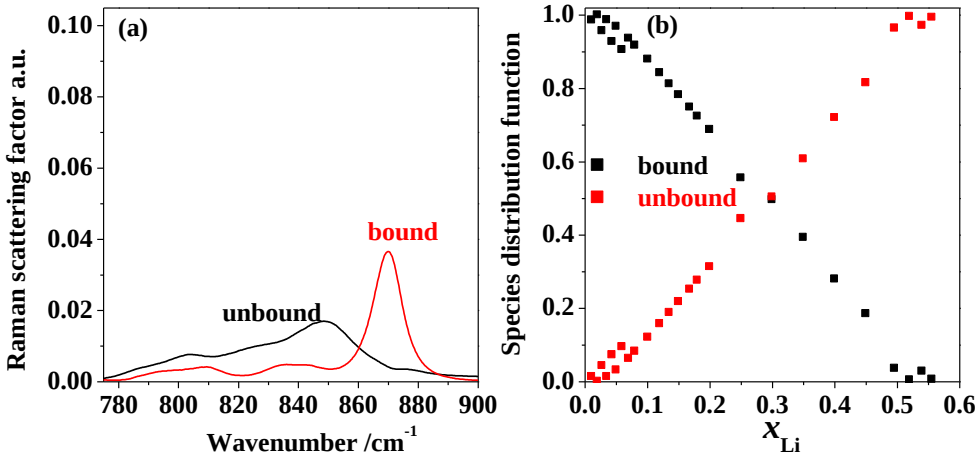

Figure S2. The Raman scattering factors (a) and species distribution functions (b) of unbound (black) and bound (red) G3 analyzed by MCR-ALS in $[LiTFSA]_x[G3]_{(1-x)}$ at 298 K in the range of 770 – 900 cm^{-1}.

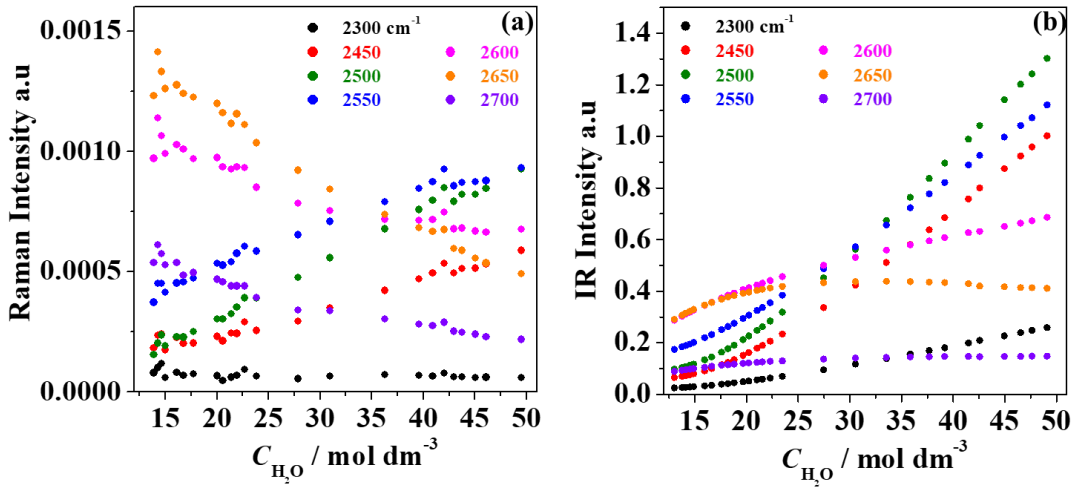

Figure S3. (a) The intensity plots of Raman spectra for H_2O in $[LiTFSA]_x[H_2O]_{(1-x)}$ at 298 K at 2300 (black), 2450 (red), 2500 (green), 2550 (blue), 2600 (pink), 2650 (orange), and 2700 (purple) cm^{-1} . (b) The intensity plots of IR spectra H_2O in $[LiTFSA]_x[H_2O]_{(1-x)}$ at 298 K at 2300 (black), 2450 (red), 2500 (green), 2550 (blue), 2600 (pink), 2650 (orange), and 2700 (purple) cm^{-1}.

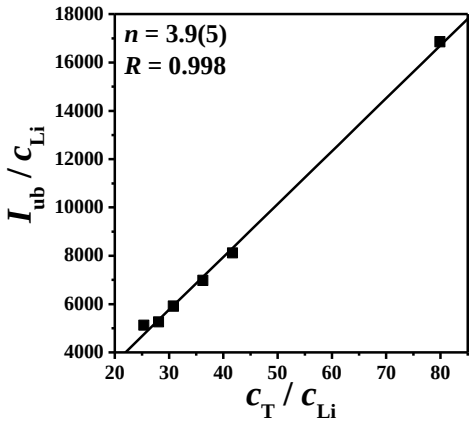

Figure S4. The plot of the intensity ratio of unbound water to Li^+ ion concentration (I_{ub} / c_{Li}) against the ratio of total water to lithium ion concentration (c_T / c_{Li}) in the concentration range c_T = 50 – 40 mol dm^{-3}.

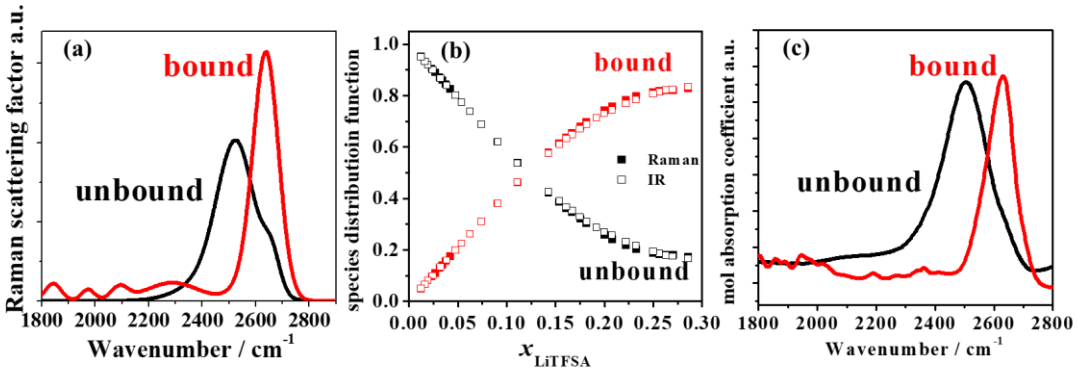

Figure S5. The Raman scattering factors (a), species distribution functions (b) and mol absorption coefficients (c) of unbound (black) and bound (red) H_2O analyzed by CLSA in $[LiTFSA]_x[H_2O]_{(1-x)}$ at 298 K in the range of 1800 – 2900 cm^{-1}. Closed squares and opened squares represent the species distribution function evaluated by Raman spectra and IR spectra, respectively.

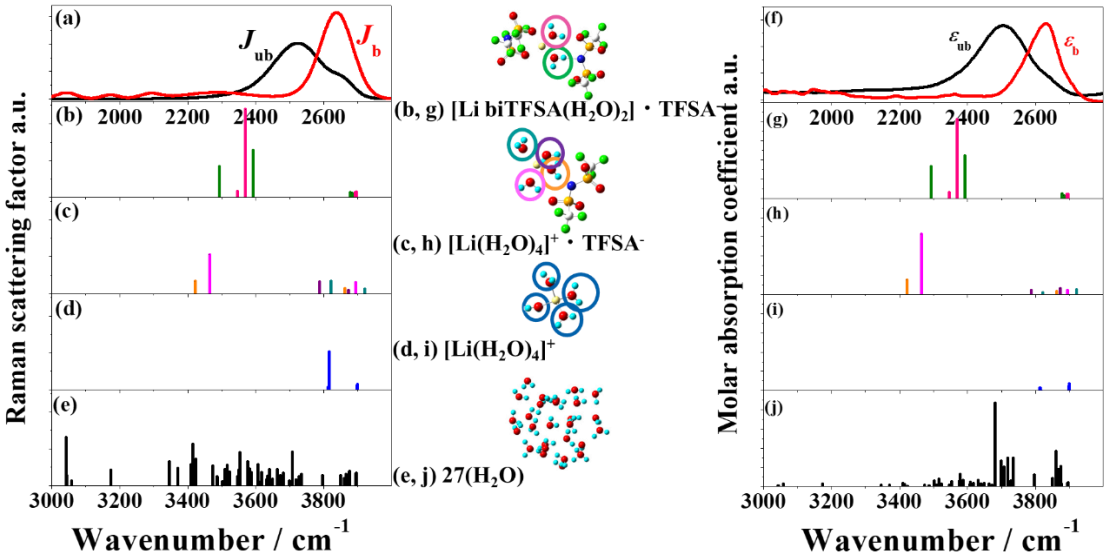

Figure S6. The Raman scattering factors (a) and the molar absorption coefficients (f) of unbound (black) and bound (red) H_2O analyzed by CLSA in $[LiTFSA]_x[H_2O]_{(1-x)}$ at 298 K in the range of 1800 – 2900 cm^{-1}. The theoretical Raman spectra (b – e) and the theoretical IR spectra (g – j) for the optimized geometries of [Li bidentate TFSA $(H_2O)_2$] $TFSA^-$ (b, g), $[Li(H_2O)_4]$ $TFSA^-$ (c, h), $[Li(H_2O)_4]$ (d, i) and $27H_2O$ (e, j), respectively.

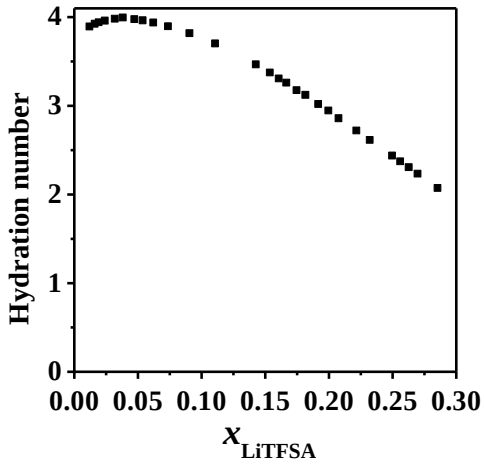

Figure S7. The plot of hydration number against the LiTFSA mole fraction.

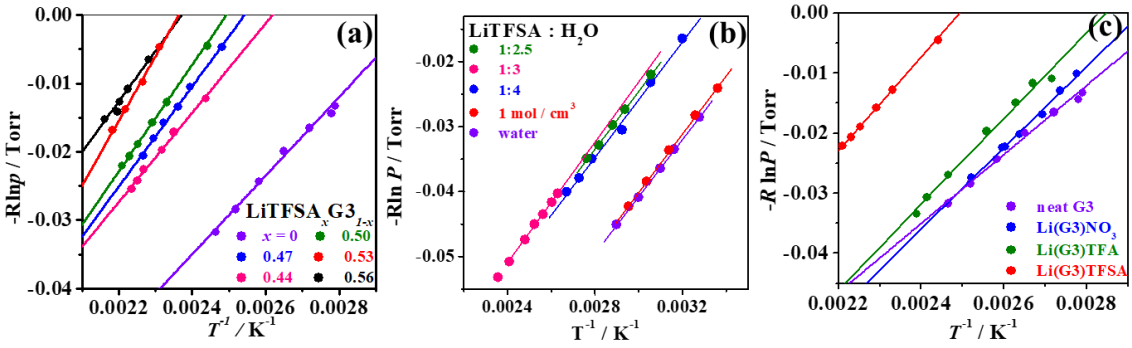

Figure S8. The plots of $-R\ln P$ against T^{-1} for $[\mathrm{LiTFSA}]_x[\mathrm{G3}]_{(1-x)}$ (a), $[\mathrm{LiTFSA}]_x[\mathrm{H_2O}]_{(1-x)}$ (b), [LiX][G3] ($\mathrm{X = NO_3^-}$, $\mathrm{TFA^-}$, $\mathrm{TFSA^-}$) (c).

Table S1. Vapor pressure at 298 K evaluated by Clausius–Clapeyron relationship, activity (α) and activity coefficient (*f*) of solvent, Gibbs free energy ΔG^o, Enthalpy ΔH^o and Entropy $T\Delta S^o$.

Sample	x_{Li}	P_{298} /kPa	α	*f*	ΔG^o /kJ mol^{-1}	ΔH^o /kJ mol^{-1}	$T\Delta S^o$ /kJ mol^{-1}
G3	0	0.093	1				
$[\mathrm{LiTFSA}]_x[\mathrm{G3}]_{(1-x)}$	0.44	0.003	0.034	0.06	-8.4(7)	-8(1)	0(2)
	0.47	0.0008	0.009	0.02	-11.8(6)	-16(1)	-4(1)
	0.5	0.0003	0.003	0.007	-14.1(6)	-20(1)	-6(1)
	0.53	0.00001	0.0001	0.0003	-22.0(7)	-37(3)	-15(3)
	0.56	0.0002	0.002	0.004	-15.7(6)	-16(2)	-1(2)
$[\mathrm{LiNO_3}]_x[\mathrm{G3}]_{(1-x)}$	0.5	0.032	0.34	0.68	-2.7(9)	-10(1)	-8(2)
$[\mathrm{LiTFA}]_x[\mathrm{G3}]_{(1-x)}$	0.5	0.013	0.14	0.28	-5(1)	-14(2)	-9(2)
$\mathrm{H_2O}$	0	20.8	1				
$[\mathrm{LiTFSA}]_x[\mathrm{H_2O}]_{(1-x)}$	0.29	3.1	0.15	0.19	-4.71(6)	-2(2)	3.3(6)
	0.25	2	0.096	0.12	-5.91(5)	-6(2)	0.1(7)
	0.2	3.4	0.16	0.19	-4.9(2)	-3(5)	2(2)
	0.091	18	0.88	0.77			